Suppressing spatially distributed disturbances by exploiting additional sensors and actuators in inferential motion control*

Nic Dirkx[a,b] (nic.dirkx@asml.com) Tom Oomen[b]
[a] *ASML Research Mechatronics & Control, Veldhoven, The Netherlands*
[b] *Eindhoven University of Technology, Control Systems Technology, Eindhoven, The Netherlands*

***Abstract*—Structural deformations resulting from exogenous disturbances limit the control performance in high-precision positioning systems. The aim of this paper is to identify these limitations and mitigate these through multivariable inferential control. A systematic analysis and control design framework is established. Herein, additional sensors and actuators are exploited to achieve control performance beyond conventional limits. Successful performance enhancement using the presented methods is shown on an identified wafer stage model.**

***Index Terms*—Inferential control, multivariable, motion systems**

I. Introduction

Structural deformations are a hampering factor in achieving the performance demands in precision positioning systems. These deformations are typically induced by non-collocated disturbances, i.e., disturbances that act at different locations than the control inputs. Examples include the disturbances induced by rollers in printing systems [1], or the immersion hood in wafer scanners [2]. Especially, the presence of spatially distributed disturbances may lead to highly complex deformations.

Structural deformations play a particularly important role when the location where performance is desired cannot be directly measured. For example, in wafer stages the performance is required at the point-of-exposure [2], while the sensors are located elsewhere in the stage. In printing systems, performance is required at the printing interface, while the sensor is typically mounted on the motor, with flexible dynamics in between [1]. In traditional motion control, the flexible dynamics between the unmeasured performance variables and the measured variables are ignored [3]. Although this leads to a simplified control problem, such approach longer suffices to meet the future performance demands.

In inferential motion control, the flexible dynamics between the measured variables and the unmeasured performance variables are addressed explicitly [6]. To control the unmeasured performance variables, these must be estimated (inferred) from the measurements. This inference requires the use of a dynamic model that includes the unmeasured performance variables and the disturbance inputs [4]. Hence, the inferential control problem is inherently a model-based control problem, and is more involved than the traditional control problem.

Particularly for multivariable problems, the explicit distinction between measured variables and performance variables, and between disturbance inputs and control inputs, has important implications for the control problem. First, the achievable inferential performance is limited by the capability of estimating and suppressing disturbances, which in turn depends on the number and placement of sensors and actuators, compared to that of the disturbances and performance variables, respectively. Second, achieving optimal disturbance estimation and suppression within these limitations requires a particularly shaped multivariable controller, which imposes specific demands on the control design methods.

The estimation and suppression of disturbances using disturbance-observer based control [7] is well-developed for problems wherein the performance variables are directly measured and the disturbances are collocated with the inputs, e.g., [8], [9]. Observer-based rejection of non-collocated disturbances is reported in, e.g., [10], for single input systems. However, since inferential control performance objectives are not addressed, these techniques do not necessarily lead to high performance in terms of the performance variables.

A $\mathcal{H}_\infty$-optimal control design approach that explicitly addresses robust inferential control performance requirements is presented in [6], though only input disturbances are considered. In [5], a $\mathcal{H}_\infty$-optimal design framework is presented for systems with non-collocated disturbances. However, limitations in the multivariable inferential control problem are not addressed in [5], [6] and hence the techniques are not generally compatible to this class of problems.

Although the inferential control problem for multivariable systems is relevant in industrial motion systems, especially in presence of spatially distributed disturbances, design methods that address these aspects explicitly are currently not available. This paper aims at improving the performance of such systems by identifying the control limitations, and mitigating these through a multivariable $\mathcal{H}_\infty$-optimal inferential control design framework. Herein, overactuation and oversensing strategies are exploited to achieve performance beyond conventional limits.

The main contributions in this paper are:

1. A framework for the analysis of sensors and actuator related performance limitations in inferential control of multivariable systems,
2. A $\mathcal{H}_\infty$-optimal observer-based inferential control design framework for multivariable systems subject to non-collocated disturbances,

*This work is part of the research programme VIDI with project number 15698, which is (partly) financed by the Netherlands Organisation for Scientific Research (NWO).

2021 IEEE International Conference on Mechatronics (ICM) | 978-1-7281-4442-9/21/$31.00 ©2021 IEEE | DOI: 10.1109/ICM46511.2021.9385648

3. A multivariable weighting filter design approach that exploits oversensing and overactuation control strategies,
4. A case study on an industrial wafer stage setup.

Proofs are omitted throughout to conserve space.

Notations: The pseudo-inverse of a matrix $X \in \mathbb{C}^{m\times n}, m \leq n$ is defined as $X^\dagger = X^H(XX^H)^{-1}$, $\sigma(X)$ denotes its singular values, and $\bar{\sigma}(X)$ the largest singular value. $\|X\|_F$ denotes the Frobenius norm. Operation $\text{blk}(X_1,\ldots,X_n)$ results in a block-diagonal matrix with $X_i,\ i=1,\ldots,n$ on the diagonal.

II. Problem Formulation

A. Inferential control problem

The linear time invariant system

$$\begin{bmatrix} z \\ y \end{bmatrix} = P \begin{bmatrix} d \\ u \end{bmatrix}, \quad P = \begin{bmatrix} P_{zd} & P_{zu} \\ P_{yd} & P_{yu} \end{bmatrix}, \tag{1}$$

is considered, where $z \in \mathbb{R}^{n_z}$ denotes the unmeasured performance variables, $y \in \mathbb{R}^{n_y}$ the measured variables, $u \in \mathbb{R}^{n_u}$ the control inputs, and $d \in \mathbb{R}^{n_d}$ the disturbances. Multivariable systems P with $n_u \leq n_z, n_y \leq n_d$ and $n_z, n_d > 1$ are considered. The considered inferential control problem is the minimization of the error $e_z = r - z$, where r is a reference signal, by design of a feedback controller $\bar{K} = [\bar{K}_r \quad \bar{K}_y]$ such that $u = \bar{K}(r, y)$. The corresponding control scheme is shown in Fig. 1.

Definition 1 (Optimal inferential controller): Given the system P, the optimal inferential controller is

$$\bar{K}^{\text{opt}} = \arg\min_{\bar{K}} \mathcal{J}(P, \bar{K}), \tag{2}$$

where $\mathcal{J}$ is the inferential control objective function.

B. System class

The following system class is considered.

Definition 2 ([13]): The motion system $P_{\star\circ}(s)$ with proportional damping can be expressed as

$$\begin{aligned} P_{\star\circ}(s) &= \sum_{i=1}^{n_{\text{rb}}} \frac{c_{\star_i}^T b_{\circ_i}}{s^2} + \sum_{j=1}^{n_{\text{flex}}} \frac{c_{\star_j}^T b_{\circ_j}}{s^2 + 2\zeta_i\omega_j s + \omega_j^2} \\ &= C_{\star_{\text{rb}}} P_{\text{rb}}(s) B_{\circ_{\text{rb}}} + C_{\star_{\text{flex}}} P_{\text{flex}}(s) B_{\circ_{\text{flex}}} \end{aligned} \tag{3}$$

is considered, where n_{rb} is the number of rigid-body modes, n_{flex} the number of flexible modes, $c_{\star_i}^T$ and $c_{\star_j}^T$ the i^{th} and j^{th} column of $C_{\star_{\text{rb}}} \in \mathbb{R}$ and $C_{\star_{\text{flex}}} \in \mathbb{R}$, respectively. Likewise, $b_{\star_i}^T$ and $b_{\star_j}^T$ are the i^{th} and j^{th} row of $B_{\star_{\text{rb}}} \in \mathbb{R}$ and $B_{\star_{\text{flex}}} \in \mathbb{R}$, respectively. Matrices $B_{\star_{\text{rb}}}$ and $C_{\star_{\text{flex}}}$ are assumed of full column and row rank, respectively. Furthermore, ζ_i and ω_i represent the damping constant and natural frequency of mode i, respectively. In view of (1), $\star$ represents y or z, while $\circ$ represents u or d.

At $s = 0$, the flexible dynamics are exactly represented by a static matrix, which is referred to as the compliance.

Definition 3: The compliance of $P_{\star\circ}(s)$ in (3) is defined as

$$\mathcal{D}_{\star\circ} \triangleq C_{\star_{\text{flex}}} P_{\text{flex}}(0) B_{\circ_{\text{flex}}} = \sum_{j=1}^{n_{\text{flex}}} \frac{c_{\star_j}^T b_{\circ_j}}{\omega_j^2}, \quad \mathcal{D}_{\star\circ} \in \mathbb{R}^{n_\star \times n_\circ}.$$

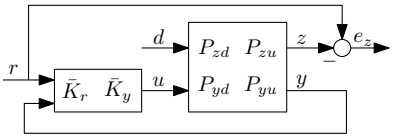

Fig. 1. General two-DOF controller structure in inferential control setup.

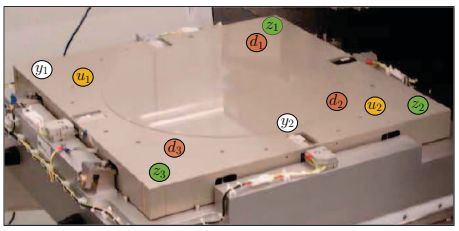

Fig. 2. Experimental setup: prototype wafer stage.

Assumption 1: For lightly damped structures, i.e., $\zeta_i \ll 1, \forall i$, the flexible dynamics are predominated by $\mathcal{D}_{\star\circ}$ over a broad frequency range, i.e, $\mathcal{D}_{\star\circ} \approx C_{\star_{\text{flex}}} P_{\text{flex}}(s) B_{\circ_{\text{flex}}}, \quad s \in [0, \alpha 2\pi j f^*]$ where f^* is the frequency [Hz] of the first resonance and $\alpha \in [0,1]$ is typically $\alpha \geq 0.5$.

C. Wafer stage setup

The inferential control problem is encountered in the control of motion platforms such as the prototype wafer stage shown in Fig. 2, which forms the experimental setup in this paper. The stage exhibits flexible dynamic behavior, and is well-represented by the system class defined in Section II-B.

In the considered configuration, the stage has a single rigid-body motion control degree-of-freedom (DOF) in the vertical direction, i.e., $n_{\text{rb}} = 1$. The stage is equipped with two actuators u_1, u_2 and two sensors y_1, y_2 in the vertical direction, as indicated in Fig. 2, and hence allows for overactuation ($n_u > n_{\text{rb}}$) and oversensing ($n_y > n_{\text{rb}}$) control strategies. The control goal is to position the three points z_1, z_2, z_3 at the three corners in Fig. 2. For validation purposes, the stage is equipped with sensor at these locations, which are not used for feedback control. In addition, three actuators are employed to apply spatially distributed disturbances d_1, d_2, d_3 in a controlled environment for evaluation purposes.

III. Control Performance Analysis Framework

In this section, a framework for the analysis of the best achievable inferential control performance for a given system is presented. Also, mitigation of performance limitations by exploiting oversensing and overactuation is investigated.

A. Minimal-spillover control

The inferential control problem imposes different requirements on the controller design and its structure than the traditional control problem wherein the measured variables are controlled directly. Consider the control scheme in Fig. 1 and the corresponding transfer function matrix (TFM) $T_{e_z} = [T_{e_z r}\ T_{e_z d}] : [r^T\ d^T]^T \mapsto e_z$,

$$\begin{bmatrix} T_{e_z r} & T_{e_z d} \end{bmatrix} = P_{zu} S_i \begin{bmatrix} \bar{K}_r & \bar{K}_y P_{yd} \end{bmatrix} + \begin{bmatrix} I & -P_{zd} \end{bmatrix} \tag{4}$$

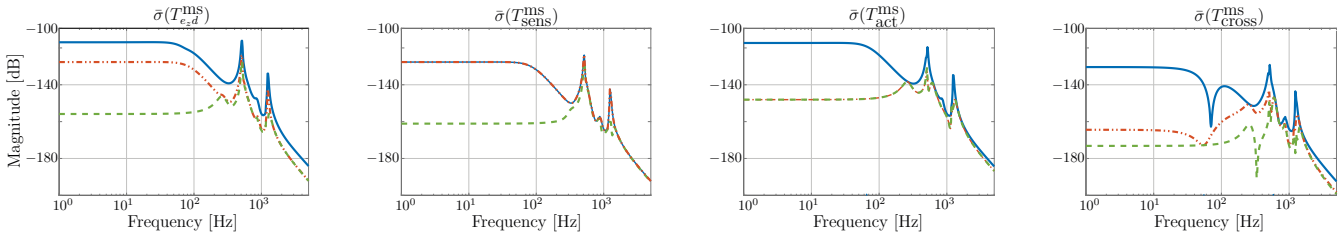

Fig. 3. Analysis of inferential control performance limitations in terms of the maximum singular values of (6) for the systems in Example 1. Low-frequency performance, i.e., $f \leq 100$Hz, is considered. The total inferential control error (*left*) for P_1 (blue solid) is dominated by actuator-induced limitations, as observed from $\bar{\sigma}(T^{\text{ms}}_{\text{act}})$ (*middle-right*). This limitation is mitigated in P_2 (red dashed-dotted) by exploiting an additional actuator, which significantly reduces $\bar{\sigma}(T^{\text{ms}}_{\text{act}})$ (*middle-right*) and hence the total error $\bar{\sigma}(T^{\text{ms}}_{e,d})$ (*left*). As expected, the sensor-induced limitations (*middle-left*) are unaffected by the additional actuator. System P_3 (green dash-dotted) also exploits an additional sensor, leading to a substantial reduction of $\bar{\sigma}(T^{\text{ms}}_{\text{sens}})$ (*middle-left*), and consequently a further reduction of the total error $\bar{\sigma}(T^{\text{ms}}_{e_z d})$ (*left*).

where $S_i = (I + \bar{K}_y P_{yu})^{-1}$. The inferential controller that minimizes (4) in the Frobenius norm is defined as the minimal-spillover controller (MSC).

Theorem 1: The non-parametric controller that minimizes $\|T_{e_z}(k)\|_F \geq \bar{\sigma}(T_{e_z}(k))$ in (4) at frequency k is the minimal-spillover controller $\bar{K}^{\text{ms}}(k)$,

$$[\bar{K}^{\text{ms}}_r(k) \quad \bar{K}^{\text{ms}}_y(k)] = \left(P_{zu}(k)P^{\dagger}_{zu}(k)\mathcal{O}^{\text{ms}}_u(k)\right)^{\dagger}[I \quad \mathcal{O}^{\text{ms}}_y(k)],$$

where $\mathcal{O}^{\text{ms}}_u(k) = P_{zu}(k) - P_{zd}(k)P^{\dagger}_{yd}(k)P_{yu}(k)$ and $\mathcal{O}^{\text{ms}}_y(k) = P_{zd}(k)P^{\dagger}_{yd}(k)$.

The MSC reveals several distinctive properties of the inferential controller compared to traditional controllers. First, the inferential controller is inherently a two-DOF controller, i.e., $\bar{K}^{\text{ms}} = [\bar{K}^{\text{ms}}_r(k) \quad \bar{K}^{\text{ms}}_y(k)]$, instead of the traditional single-DOF controller. Second, its dynamics depend on all four blocks of the plant P, while the traditional control problem simply requires high-gain control [5]. Third, the MSC intrinsically contains a minimal spillover observer $\mathcal{O}^{\text{ms}} : \hat{z} = [\mathcal{O}^{\text{ms}}_u \quad \mathcal{O}^{\text{ms}}_y][u_o^T \quad y^T]^T$ that estimates the performance variables z subject to disturbances d, from signals u_o and y, with u_o the unperturbed control signa, as in Fig. 4. Theorem 1 extends the results for zero-spillover control in SISO systems [11] to multivariable systems with possibly non-square dimensions.

Remark 1: The MSC is a non-parametric controller and serves the purpose of facilitating design and analysis rather than actual implementation.

The concept of the MSC gives rise to a systematic performance analysis framework. This is presented in the next section.

B. Identification of fundamental performance limitations

The MSC concept enables analysis of best achievable performance and the identification of performance limitations. Inserting $\bar{K}^{\text{ms}}$ into (4) leads to an expression for the theoretically best achievable inferential control performance,

$$T^{\text{ms}}_{e_z} = [I - P_{zu}P^{\dagger}_{zu} \quad P_{zd} - P_{zu}P^{\dagger}_{zu}P_{zd}P^{\dagger}_{yd}P_{yd}]. \tag{5}$$

To pinpoint the fundamental bottlenecks in achieving high-performance control, consider the following result.

Lemma 2: The sub-block $T^{\text{ms}}_{e_z d} : d \mapsto e_z$ in (5) is decomposed as

$$T^{\text{ms}}_{e_z d} = T^{\text{ms}}_{\text{sens}} + T^{\text{ms}}_{\text{act}} + T^{\text{ms}}_{\text{cross}}, \tag{6}$$

with

$$\begin{aligned} T^{\text{ms}}_{\text{sens}} &= P_{zd}(I_{n_d} - P^{\dagger}_{yd}P_{yd}) \\ T^{\text{ms}}_{\text{act}} &= \quad (I_{n_z} - P_{zu}P^{\dagger}_{zu})P_{zd} \\ T^{\text{ms}}_{\text{cross}} &= -(I_{n_z} - P_{zu}P^{\dagger}_{zu})P_{zd}(I_{n_d} - P^{\dagger}_{yd}P_{yd}), \end{aligned} \tag{7}$$

where $\text{rank}(T^{\text{ms}}_{\text{sens}}) = \min(n_z, n_d - n_y)$ and $\text{rank}(T^{\text{ms}}_{\text{act}}) = \min(n_d, n_z - n_u)$.

Term $T^{\text{ms}}_{\text{sens}}$ represents the error contribution originating from a potentially insufficient number of sensors n_y to estimate the n_d disturbances. By duality, term $T^{\text{ms}}_{\text{act}}$ represents the contribution originating from a potentially insufficient number of actuators n_u to control the n_z performance variables, i.e., $\text{rank}(T^{\text{ms}}_{\text{act}}) = \min(n_d, n_z - n_u)$. Term $T^{\text{ms}}_{\text{cross}}$ represents a cross-contribution due to the aforementioned limitations.

The above analysis motivates the use of additional sensors and actuators. This is investigated in the next section.

C. Improving performance by oversensing and overactuation

The presented analysis framework facilitates making control system design choices on sensor and actuator placement. Mitigation of the fundamental performance limitations by means of oversensing and overactuation is investigated in the following example.

Example 1: Consider models P_1, P_2, P_3 of the wafer stage described in Section II-C. P_1 employs sensor y_1 and actuator u_1 only. To study overactuation, both actuators u_1, u_2 are included in model P_2. To additionally study oversensing, both actuators u_1, u_2 and sensors y_1, y_2 are included in model P_3. The decomposition of $T^{\text{ms}}_{e_z d}$ in (6) is shown in Fig. 3.

The presented concepts are exploited in the design of $\mathcal{H}_\infty$-optimal inferential controller design in the following sections.

IV. $\mathcal{H}_\infty$-Optimal Observer-Based Inferential Control Design Framework

This section presents the $\mathcal{H}_\infty$-optimal observer-based inferential controller design framework.

A. Controller structure selection

Various implementations of two-DOF controllers exist [12, p. 147]. In this paper, the observer-based controller is considered, see the dashed box in Fig. 4, as it provides an intuitive two-DOF structure for inferential control for two reasons.

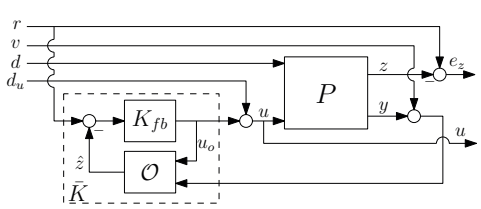

Fig. 4. Generalized inputs and outputs

First, the MSC contains a minimal spillover observer $\mathcal{O}^{\text{ms}}$, as shown in Theorem 1. Second, the separation in an observer and controller intuitively connects to the decomposition in (6), where $T_{\text{sens}}^{\text{ms}}$ is due the observer error, and $T_{\text{act}}^{\text{ms}}$ is due to the controller error.

The two-DOF observer-based controller is expressed as

$$\bar{K}(\mathcal{O}, K_{fb}): \quad u = S_{\mathcal{O}} K_{fb} \begin{bmatrix} I & -\mathcal{O}_y \end{bmatrix} \begin{bmatrix} r \\ y \end{bmatrix}, \tag{8}$$

where $S_{\mathcal{O}} = (I + K_{fb}\mathcal{O}_u)^{-1}$, with K_{fb} the feedback controller and $\mathcal{O}$ the observer,

$$\mathcal{O}: \quad \hat{z} = \begin{bmatrix} \mathcal{O}_u & \mathcal{O}_y \end{bmatrix} \begin{bmatrix} u \\ y \end{bmatrix}, \tag{9}$$

with $\hat{z}$ an estimate of the performance variable z.

B. Inferential control goal

The design of $\mathcal{H}_\infty$-optimal controllers requires the selection of the generalized inputs and outputs such that the control criterion in (2) reflects the control goal. The presented selection is shown in Fig. 4 and is motivated as follows: inputs r, d are the inputs that must be tracked or suppressed, respectively. Input v is included to enable high-frequency controller roll-off properties, and d_u is included to bound the input sensitivity function S_i, i.e., to include robustness margins. Output e_z is the inferential control error and u is the control command that should remain bounded. This selection results in the closed-loop TFM $T(P, \mathcal{O}, K_{fb}) : \bar{w} \mapsto \bar{z}$,

$$T = \begin{bmatrix} -P_{zu} \\ I \end{bmatrix} S_i [\bar{K}_r \;\; \bar{K}_y \;\; -\bar{K}_y P_{yd} \;\; I] + \begin{bmatrix} I & 0 & -P_{zd} & 0 \\ 0 & 0 & 0 & 0 \end{bmatrix} \tag{10}$$

where

$$\bar{w}^T = \begin{bmatrix} r^T & v^T & d^T & d_u^T \end{bmatrix}^T, \quad \bar{z}^T = \begin{bmatrix} e_z^T & u^T \end{bmatrix}^T.$$

The TFM T in (10) is an eight-block problem and extends upon the traditional four-block problem, e.g., [14].

To specify performance requirements, the weighting matrices

$$W = \text{blk}(W_z, W_u), \quad V = \text{blk}(V_r, V_v, V_d, V_{d_u}), \tag{11}$$

are introduced, where $W, V \in \mathcal{RH}_\infty$, such that $w = V\bar{w}$ and $z = W\bar{z}$. The control criterion (2) is then defined as

$$\mathcal{J}(P, \mathcal{O}, K_{fb}) = \left\| W T(P, \mathcal{O}, K_{fb}) V \right\|_\infty. \tag{12}$$

C. Inferential-control-relevant observer design

To achieve optimal control performance, the observer is designed directly in view of criterion (12), leading to the inferential-control-relevant (ICR) observer.

Definition 4 (ICR observer [5]): For a given controller K_{fb}, the ICR observer is computed by

$$\mathcal{O}^{\text{ICR}}(P, K_{fb}) = \arg\min_{\mathcal{O}} \mathcal{J}(P, \mathcal{O}, K_{fb}). \tag{13}$$

The resulting observer-based controller of form (8) and hence the achieved control cost is invariant under any choice of biproper, minimum phase and full rank K_{fb} [5].

In the next section, a method for the design of multivariable weighting filters W, V is presented that reflects desired performance requirements and addresses the performance limitations in multivariable inferential control.

V. Multivariable Weighting Filter Design

The design of weighting matrices W, V in (11) is significantly more involved for the multivariable inferential control problem than for the classical control problem, because

(i) the inferential controller generally has coupled multivariable dynamics, and so traditional multiloop SISO weighting filter design approaches [3] cannot be applied,
(ii) traditional desired loop shapes [3], [12] that impose offset-free control are no longer sensible in case offset-free control is prohibited by sensor and actuator induced performance limitations.

In this section, a multivariable weighting filter design approach is presented that addresses issues (i-ii). The key idea is to shape the $\mathcal{H}_\infty$-optimal controller towards the MSC, as defined in Section III. The design approach accommodates the use of additional sensors and actuators.

A. Closed-loop shape requirements

Weighting filter design typically aims at specifying low-frequency and high-frequency asymptotes of certain entries of T in (10). Particularly, the following requirements are pursued.

Definition 5 (Closed-loop shape requirements):

R1 Reference tracking requires a small gain of $\bar{\sigma}(T_{e_z r})$, with $T_{e_z r} : r \mapsto e_z$, below f_r, i.e., $\bar{\sigma}(T_{e_z r}) \ll 1 \; \forall f \in [0, f_r]$.
R2 For disturbance suppression, a small gain of $\bar{\sigma}(T_{e_z d})$ must be attained below f_d, i.e., $\bar{\sigma}(T_{e_z d}) \ll 1 \; \forall f \in [0, f_d]$.
R3 Controller roll-off requires a small gain of $\bar{\sigma}(T_{uv})$ with $T_{uv} : v \mapsto u$ beyond f_c, i.e., $\bar{\sigma}(T_{uv}) \ll 1 \; \forall f \in [f_c, f_\infty]$.

B. Design procedure

This section presents a multivariable weighting filter design approach that enables shaping the $\mathcal{H}_\infty$-optimal controller towards the MSC, as defined in Section III. The design approach consists in three steps:

1) Nullspace alignment (na)
2) Scaling (sc)
3) Loopshaping (ls).

The weighting filters are composed accordingly, i.e.,

$$W = W^{\text{ls}} W^{\text{sc}} W^{\text{na}}, \quad V = V^{\text{na}} V^{\text{sc}} V^{\text{ls}}. \tag{14}$$

1) Nullspace Alignment: The MSC provides a template for the multivariable $\mathcal{H}_\infty$-optimal inferential controller. Therefore, a weighting filter design approach is pursued that results in a controller that approximates the MSC in the frequency range of interest, i.e., the low-frequency range $f \in [0, \max(f_r, f_d)]$ as specified in requirements R1 and R2. This is achieved by imposing offset-free control in those input and output directions in which offset-free control is achieved by the MSC. These directions are associated to the left and right nullspaces of $T^{\text{ms}}_{\text{act}}$ and $T^{\text{ms}}_{\text{sens}}$ in (6), respectively. Step 1 in the design approach therefore consists in an alignment with these nullspace directions. Consider the following rotation matrix.

Definition 6: The right nullspace alignment (RNA) matrix is defined as $\mathcal{V} = \text{im}(F_{yd}),\ \mathcal{V} \in \mathbb{R}^{n_d \times n_y}$, where

$$F_{yd} = \left[\begin{array}{cc} \mathcal{D}_{yd}^T (I_{n_y} - C_{y_{\text{rb}}} C_{y_{\text{rb}}}^\dagger) & B_{d_{\text{rb}}}^T \end{array} \right]. \tag{15}$$

And consider the dual definition.

Definition 7: The left nullspace alignment (LNA) matrix is defined as $\mathcal{U} = \text{im}(F_{zu})^T,\ \mathcal{U} \in \mathbb{R}^{n_u \times n_z}$, where

$$F_{zu} = \left[\begin{array}{cc} \mathcal{D}_{zu} (I_{n_u} - B_{u_{\text{rb}}}^\dagger B_{u_{\text{rb}}}) & C_{z_{\text{rb}}} \end{array} \right]. \tag{16}$$

As discussed in Section III, the nullspace dimensions of $T^{\text{ms}}_{\text{act}}$ and $T^{\text{ms}}_{\text{sens}}$ in (6) depend on the degree of actuation and sensing, respectively. This dependence is reflected in the RNA and LNA matrices. More precisely, $\mathcal{D}_{yd}^T (I_{n_y} - C_{y_{\text{rb}}} C_{y_{\text{rb}}}^\dagger)$ represents a rank $n_y - n_{\text{rb}}$ metric of the disturbance-induced deformations that can be estimated from the sensors, whereas $\mathcal{D}_{zu}(I_{n_u} - B_{u_{\text{rb}}}^\dagger B_{u_{\text{rb}}})$ represents a rank $n_u - n_{\text{rb}}$ metric of the deformations that can be actuated to control the unmeasured performance variables. Hereby, oversensing and overactuation is explicitly addressed in the nullspace alignment step.

Now, consider the following result.

Lemma 3: Consider the coordinate transformations $d = \mathcal{V}\delta$, $\mu = \mathcal{U}z$ and $r = \mathcal{U}^T r_\mu$ with $\mathcal{V}$ and $\mathcal{U}$ as in Definition 6 and 7, respectively, and define,

$$T^{\text{ms}}_{e_\mu} : \left[\begin{array}{c} r_\mu \\ \delta \end{array} \right] \mapsto e_\mu = \mathcal{U}\ T^{\text{ms}}_{e_z} \left[\begin{array}{cc} \mathcal{U}^T & 0 \\ 0 & \mathcal{V} \end{array} \right]. \tag{17}$$

with $T^{\text{ms}}_{e_z}$ given by (5). Then, $T^{\text{ms}}_{e_\mu}(0) = 0_{n_\mu \times n_\delta}$.

Lemma 3 verifies that the coordinate transformation exposes the offset-free control directions of the MSC. In turn, this implies that imposing offset-free control in these directions in the $\mathcal{H}_\infty$-optimal controller design problem results in a controller that is equal to the MSC at $s = 0$. To this end, the coordinate transformation is incorporated in the weighting filters (14) as

$$W^{\text{na}} = \text{blk}(\mathcal{U}, I_{n_u}), \quad V^{\text{na}} = \text{blk}(\mathcal{U}^T, I_{n_y}, \mathcal{V}, I_{n_u}). \tag{18}$$

Even though Lemma 3 applies only at $s = 0$, by virtue of Assumption 1, the realized coordinate transformation is accurate over a broad frequency range, i.e., for $T^{\text{ms}}_{e_\mu}(f) \approx 0_{n_\mu \times n_\delta},\ f \in [0, \alpha f^*]$. This enables approximation of the MSC over a broader frequency range.

The nullspace-aligned system $T^{\text{na}} = W^{\text{na}} T V^{\text{na}}$ forms the basis for the subsequent scaling and loop shaping steps.

2) Scaling: The goal of scaling is to balance the magnitudes of T^{na} at the target bandwidth.

Definition 8 (Bandwidth): The bandwidth f_{bw} is the frequency where $\bar{\sigma}(\bar{K}_y P_{yu})$ first crosses 1 from above.

This is achieved by choosing

$$\left[\begin{array}{c} W_z^{\text{sc}} \\ W_u^{\text{sc}} \end{array} \right] = \left[\begin{array}{c} I_{n_\mu} \\ \bar{\sigma}(P_{zu}(f_{bw})) I_{n_u} \end{array} \right], \quad \left[\begin{array}{c} V_r^{\text{sc}} \\ V_v^{\text{sc}} \\ V_d^{\text{sc}} \\ V_{d_u}^{\text{sc}} \end{array} \right] = \left[\begin{array}{c} \frac{1}{\bar{\sigma}(P_{zu}(f_{bw}))} I_{n_\mu} \\ I_{n_y} \\ \frac{1}{\bar{\sigma}(P_{zd}(f_{bw}))} I_{n_\delta} \\ I_{n_u} \end{array} \right]$$

The resulting system $T^{\text{sc}} = W^{\text{sc}} T^{\text{na}} V^{\text{sc}}$ forms a convenient basis for loop shaping in the next step.

3) Loop-shaping: Let $H_{LP}(f_1)$ and $H_{HP}(f_1)$ be biproper first-order normalized low-pass and high-pass filters, respectively, with corner frequency f_1. Then, the following weighting functions reflect the requirements R1-R3:

$$\left[\begin{array}{c} W_z^{\text{ls}} \\ W_u^{\text{ls}} \end{array} \right] = \left[\begin{array}{c} I_{n_\mu} \\ \frac{H_{LP}(f_d)}{H_{HP}(f_c)} I_{n_u} \end{array} \right], \quad \left[\begin{array}{c} V_r^{\text{ls}} \\ V_v^{\text{ls}} \\ V_d^{\text{ls}} \\ V_{d_u}^{\text{ls}} \end{array} \right] = \left[\begin{array}{c} \frac{1}{H_{LP}(f_r)} I_{n_\mu} \\ I_{n_y} \\ \frac{1}{H_{LP}(f_d)} I_{n_\delta} \\ H_{HP}(f_c) I_{n_u} \end{array} \right].$$

Here, V_r^{ls} and V_d^{ls} impose offset-free reference tracking and disturbance suppression, respectively, in terms of the transformed coordinates μ and δ in Lemma 3. W_u^{ls} enforces high-frequency controller roll-off. $V_{d_u}^{\text{ls}}$ is required for a feasibly weighted problem. The characteristic frequencies f_r, f_d, f_c are typically expressed as a (fixed) factor or fraction of the bandwidth f_{bw} [3].

Applying the presented three-step design approach leads to a $\mathcal{H}_\infty$-optimal controller that is shaped as the MSC $\bar{K}^{\text{ms}}$ in the low-frequency range. This is illustrated in the wafer stage study in the next section.

VI. Case Study

The developed framework is validated in a case study based on a measured frequency response model of the wafer stage setup in Section II-C.

A. Sensor and actuator configurations

Three cases are considered, which differ in the selection of sensors and actuators, see Fig. 2, used for feedback control:

C1) Conventional: only actuator u_1 and sensor y_1 are used.
C2) Overactuation: actuators u_1, u_2 and sensor y_1 are used.
C3) Overactuation & oversensing: actuators u_1, u_2 and sensors y_1, y_2 are used.

B. Controller designs

For all cases, the ICR observers in (13) are obtained through $\mathcal{H}_\infty$-optimization [12], based on a model of P and a PID controller K_{fb} that achieves a 40Hz bandwidth, in terms of $\bar{\sigma}(K_{fb} P_{yu})$. The weighting filters are designed according to Section V, with characteristic frequencies $f_{bw} = 40, f_r = f_d = 20, f_c = 200$. The synthesis leads to the $\mathcal{H}_\infty$-optimal controllers $\bar{K}$ of the form (8). To compare performance with traditionally designed controllers, a set of $\mathcal{H}_\infty$-optimal controllers $\bar{K}^{\text{trad}}$ is synthesized that aim to minimize the measured variables under input disturbances [3]. The singular

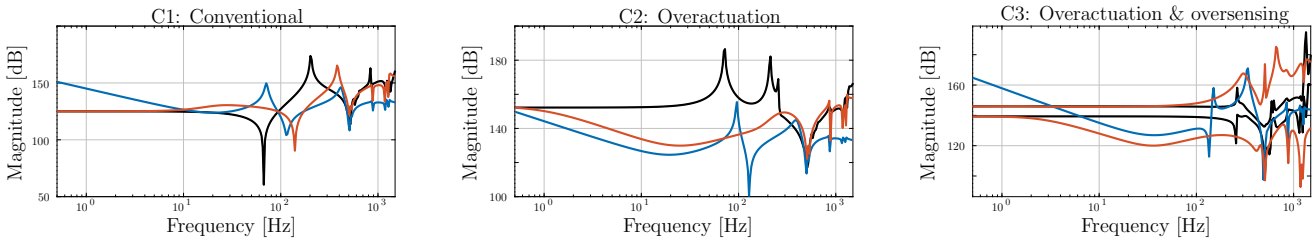

Fig. 5. Singular values of the different controllers for cases C1-C3. In all cases, the $\mathcal{H}_\infty$-optimal controllers $\bar{K}_y$ (red) better approximate the MSCs $\bar{K}_y^{\text{ms}}$ (black), than the traditional controllers $\bar{K}_y^{\text{trad}}$ (blue).

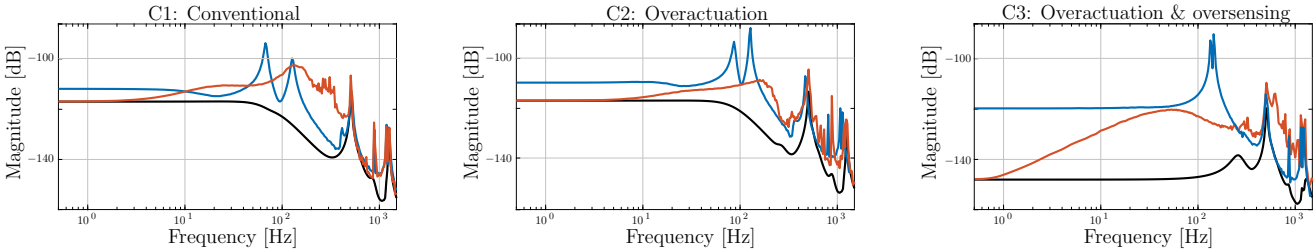

Fig. 6. Maximum singular values of $T_{e_z d}$ achieved by the different controllers for cases C1-C3. In all cases, the performance achieved by controllers $\bar{K}_y$ (red) accurately approaches the best achievable performance (black) at low frequencies, in contrast to the traditional controllers $\bar{K}_y^{\text{trad}}$ (blue).

values of the controllers $\bar{K}_y$ and $\bar{K}_y^{\text{trad}}$ are depicted in red and blue in Fig. 5, respectively, together with those of the MSC $\bar{K}_y^{\text{ms}}$ in black. At $s = 0$, the controller gains of $\bar{K}_y$ match with $\bar{K}_y^{\text{ms}}$, and additionally the dynamics approximate those of $\bar{K}_y^{\text{ms}}$ well at low frequencies. This demonstrates the effect of the presented multivariable weighting design procedure. In contrast, the traditional controllers $\bar{K}^{\text{trad}}$ have integral action and hence do not match with the MSC gain.

C. Closed-loop performance analysis

The achieved closed-loop control performance in terms of $\bar{\sigma}(T_{e_z d})$ is shown in Fig. 6. For all three cases, the controllers $\bar{K}_y$ (red) achieve the same performance level as the MSC $\bar{K}_y^{\text{ms}}$ (black) at $s = 0$. Furthermore, in the low frequency region, the singular values achieved by $\bar{K}_y$ approximate those achieved by the MSC. This illustrates the effectiveness of the presented multivariable design procedure. In contrast, the traditional controller $\bar{K}^{\text{trad}}$ is substantially less capable of suppressing the disturbances.

Comparing among the different cases, a clear reduction of the maximum singular values is observed using overactuation (C2) compared to when using conventional actuation (C1). Applying oversensing in addition (C3), the singular values are reduced further. This demonstrates the role of overactuation and oversensing in improving inferential control performance, and verifies the multivariable design approach as presented in this paper.

VII. Conclusions

An inferential control design framework is presented that enables improving the control performance of high-precision multivariable positioning systems. This is achieved by a control design framework that explicitly addresses the effect of spatially distributed external disturbances on the performance variables. In addition, the framework exploits the employment of oversensing and overactuation strategies to mitigate sensor and actuator-related fundamental performance limitations. Results from a wafer stage model verify that high control performance is achieved using the presented techniques.

References

[1] Winarto R, Koekebakker S, Steinbuch M. Combining ILC and repetitive control to handle repeating, event-triggered disturbances in precision inkjet printing. Proc. of the ACC. 3613-3618, 2015

[2] Butler H, Position control in lithographic equipment. An enabler for current-day chip manufacturing. IEEE Control Systems Magazine, 31(5):28-47, 2011.

[3] van de Wal M, van Baars G, Sperling F, Bosgra O. Multivariable $\mathcal{H}_\infty/\mu$ feedback control design for high-precision wafer stage motion. Control Engineering Practice. 10:739-755, 2002.

[4] Parrish J, Brosilow C. Inferential control applications. Automatica. 21(5), 1985.

[5] Dirkx N, Mooren N, Oomen T, Suppressing non-collocated disturbances in inferential motion control: with application to a wafer stage. Submitted, 2020.

[6] Oomen T, Grassens E, Hendriks F. Inferential Motion Control: Identification and Robust Control Framework for Positioning an Unmeasurable Point of Interest. IEEE TCST. 23(4): 1602-1610, 2015.

[7] Chen W, Yang L, Guo L, Li S. Disturbance-Observer-Based Control and Related Methods—An Overview. IEEE T. Ind. Electron. 62(2): 1083-1095, 2016.

[8] Schrijver E, Dijk J. Disturbance Observers for Rigid Mechanical Systems: Equivalence, Stability, and Design. J. Dyn. Syst. Meas. Control. 124: 539-548, 2002.

[9] Han J. From PID to Active Disturbance Rejection Control. IEEE T. Ind. Electron. 56(3): 900-906, 2009.

[10] Sariyildiz E, Mutlu, R, Zhang C. Active Disturbance Rejection Based Robust Trajectory Tracking Controller Design in State Space. ASME J.Dyn. Sys., Meas., Control, 2019

[11] Hong J, Bernstein D. Bode integral constraints, collocation, and spillover in active noise and vibration control. IEEE TCST. 6(1): 111-120, 1998.

[12] Skogestad S, Postlethwaite I. Multivariable Feedback Control: Analysis and Design. John Wiley & Sons, Inc, Hoboken, USA; 2005.

[13] Gawronksi W. Advanced structural dynamics and active control of structures. Springer, New York, New Yoirk, USA, 2004.

[14] McFarlane D, Glover K. Robust Controller Design Using Normalized Coprime Factor Plant Descriptions, ser. LNCIS. Berlin, Germany: Springer-Verlag. vol. 138, 1990.